Materials Today Bio 26 (2024) 101050

Contents lists available at ScienceDirect

Materials Today Bio

journal homepage: www.journals.elsevier.com/materials-today-bio

Cyclic stretch induced epigenetic activation of periodontal ligament cells

Han-Jin Bae [a,b,c,1], Seong-Jin Shin [a,c,1], Seung Bin Jo [a], Cheng Ji Li [a,b,c], Dong-Joon Lee [a,d], Jun-Hee Lee [a,b,c,e,f], Hae-Hyoung Lee [a,b,g,h], Hae-Won Kim [a,b,c,e,f,g,h,**], Jung-Hwan Lee [a,b,c,f,g,h,*]

[a] Institute of Tissue Regeneration Engineering (ITREN), Dankook University, Cheonan, 31116, Republic of Korea
[b] Department of Nanobiomedical Science and BK21 PLUS NBM Global Research Center for Regenerative Medicine, Dankook University, Cheonan, 31116, Republic of Korea
[c] Mechanobiology Dental Medicine Research Center, Dankook University, Cheonan, 31116, Republic of Korea
[d] Department of Oral Histology, College of Dentistry, Dankook University, Cheonan, 31116, Republic of Korea
[e] Department of Regenerative Dental Medicine, College of Dentistry, Dankook University, Cheonan, 31116, Republic of Korea
[f] Cell & Matter Institute, Dankook University, Cheonan, 31116, Republic of Korea
[g] Department of Biomaterials Science, College of Dentistry, Dankook University, Cheonan, 31116, Republic of Korea
[h] UCL Eastman-Korea Dental Medicine Innovation Centre, Dankook University, Cheonan, 31116, Republic of Korea

ARTICLE INFO

Keywords:
Biophysical cues
Periodontal ligament cell
Lineage specification
Euchromatin status

ABSTRACT

Periodontal ligament (PDL) cells play a crucial role in maintaining periodontal integrity and function by providing cell sources for ligament regeneration. While biophysical stimulation is known to regulate cell behaviors and functions, its impact on epigenetics of PDL cells has not yet been elucidated. Here, we aimed to investigate the cytoskeletal changes, epigenetic modifications, and lineage commitment of PDL cells following the application of stretch stimuli to PDL. PDL cells were subjected to stretching (0.1 Hz, 10 %). Subsequently, changes in focal adhesion, tubulin, and histone modification were observed. The survival ability in inflammatory conditions was also evaluated. Furthermore, using a rat hypo-occlusion model, we verified whether these phenomena are observed *in vivo*. Stretched PDL cells showed maximal histone 3 acetylation (H3Ace) at 2 h, aligning perpendicularly to the stretch direction. RNA sequencing revealed stretching altered gene sets related to mechanotransduction, histone modification, reactive oxygen species (ROS) metabolism, and differentiation. We further found that anchorage, cell elongation, and actin/microtubule acetylation were highly upregulated with mechanosensitive chromatin remodelers such as H3Ace and histone H3 trimethyl lysine 9 (H3K9me3) adopting euchromatin status. Inhibitor studies showed mechanotransduction-mediated chromatin modification alters PDL cells behaviors. Stretched PDL cells displayed enhanced survival against bacterial toxin (C12-HSL) or ROS (H_2O_2) attack. Furthermore, cyclic stretch priming enhanced the osteoclast and osteoblast differentiation potential of PDL cells, as evidenced by upregulation of lineage-specific genes. *In vivo*, PDL cells from normally loaded teeth displayed an elongated morphology and higher levels of H3Ace compared to PDL cells with hypo-occlusion, where mechanical stimulus is removed. Overall, these data strongly link external physical forces to subsequent mechanotransduction and epigenetic changes, impacting gene expression and multiple cellular behaviors, providing important implications in cell biology and tissue regeneration.

1. Introduction

Recent research at the interface of cell biology and biomedical engineering has underscored the pivotal role of mechanical forces in modulating cell function and fate [1,2]. Forces including tension, compression, and shear stress precisely regulate vital cell processes like proliferation, differentiation, and apoptosis [3–5]. In this rapidly expanding field, concerted efforts are underway to elucidate the intricate interplay between mechanical forces and intracellular components that gives rise to tailored cellular responses [6,7]. However, despite

* Corresponding author. Institute of Tissue Regeneration Engineering (ITREN), Dankook University, Cheonan, 31116, Republic of Korea.
** Corresponding author. Institute of Tissue Regeneration Engineering (ITREN), Dankook University, Cheoan, 31116, Republic of Korea.
E-mail addresses: bhj137@naver.com (H.-J. Bae), ko2742@naver.com (S.-J. Shin), kimhw@dku.edu (H.-W. Kim), ducious@gmail.com (J.-H. Lee).
[1] Contributed equally to this work as first authors.

https://doi.org/10.1016/j.mtbio.2024.101050
Received 3 January 2024; Received in revised form 25 March 2024; Accepted 8 April 2024
Available online 12 April 2024

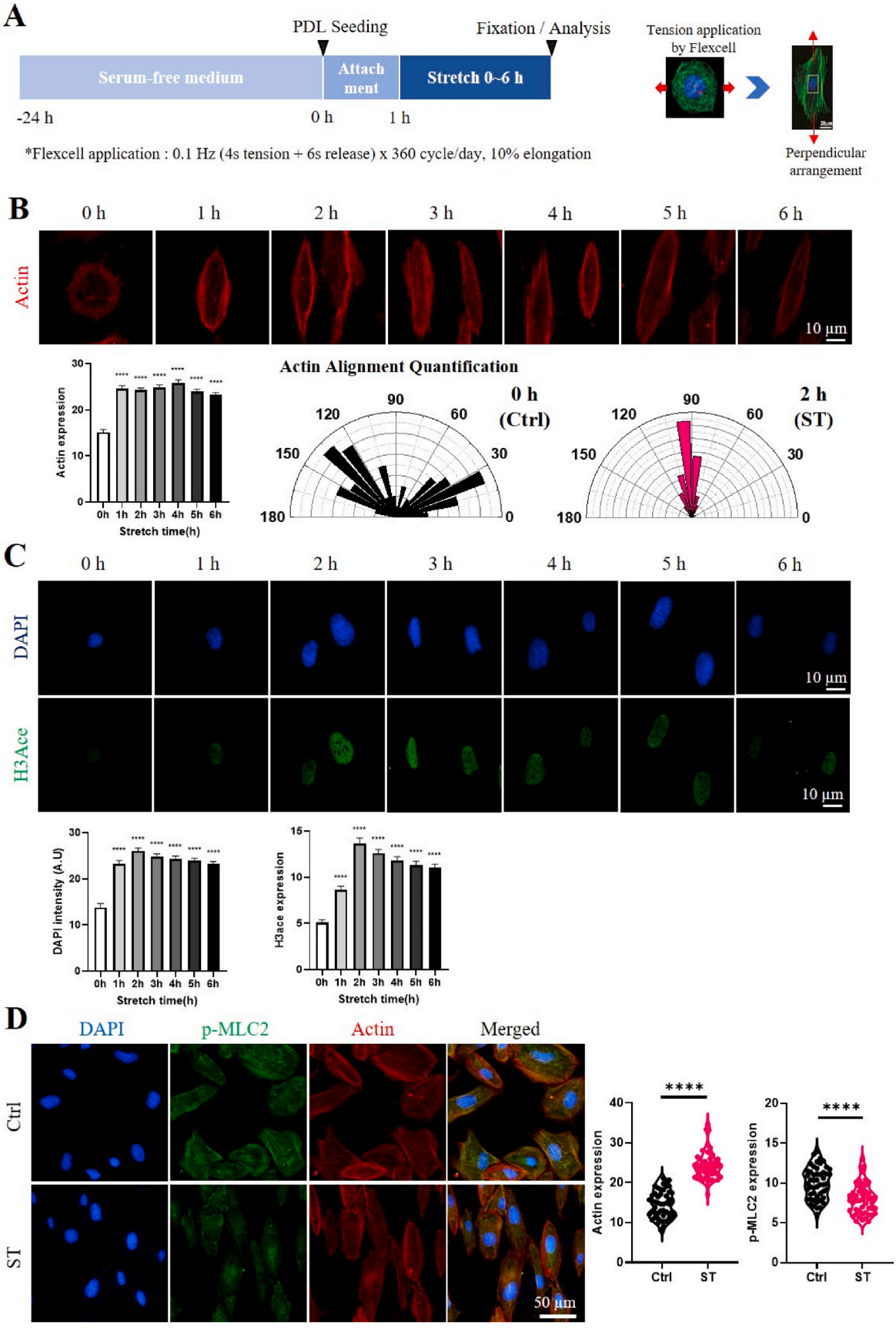

(caption on next page)

Fig. 1. Stretch-induced cellular responses and chromatin remodeling in periodontal ligament cells. (**A**) Schematic of experimental setup time point for mechanical stretch application. Cells were cultured in serum-free medium for 24 h, seeded on flexcell plates, and applied stretch from 0 to 6 h after 1 h. (**B**) Immunostaining of actin cytoskeletons under stretch from 0 to 6 h. Quantification analysis of actin expression reveals that expression levels are significantly higher in stretch than in 0 h (Ctrl), and cell alignment appears only in stretch (ST) group but not in Ctrl group. Quantification of cell alignment was presented as a rose plot of actin cytoskeleton orientation. All groups compared with 0 h. Triplicate biological experiments were performed and representative data from 50 cells were depicted. (**C**) Immunofluorescence imaging of DAPI-stained nucleus and H3Ace under stretch from 0 to 6 h. Quantitative analysis of DAPI and H3Ace expression indicated that expression levels were significantly higher in stretch compared with 0 h (Ctrl). All groups were compared to 0 h. Triplicate biological experiments were performed and representative data from 50 cells were depicted. (**D**) Immunofluorescence images of p-MLC2 in Ctrl (0 h) and ST 2 h. Quantitative analysis of p-MLC2 and actin expression was significantly higher in ST compared to Ctrl. Triplicate biological experiments were performed and representative data from 50 cells were depicted. $^{****}P < 0.0001$, ns; not significant, one-way ANOVA with Tukey's post hoc test or unpaired *t*-test. All bar plots show mean value ± SEM. Ctrl; control group, without stretch ST; stretch induced group.

meaningful advances, gaps remain in fully elucidating the subtle spatiotemporal dynamics between forces and cell machineries. Further interrogation of these complex biological systems through multi-disciplinary approaches is therefore imperative to gain a predictive understanding of mechanotransduction events across scales.

Mechanotransduction, the process by which mechanical cues are transduced into biochemical signals to regulate downstream gene and protein expression governing cellular function, has emerged as a fundamental paradigm for understanding cell-matrix interactions [8–10]. This intricate machinery encompasses several major components spanning the cell membrane, cytosolic compartments, and even intranuclear space [3,11]. Key contributors such as focal adhesions, cytoskeletal elements, and the nuclear envelope (lamins) collectively facilitate communication between the extracellular matrix niche and the genome to activate mechanoresponsive programs [6,12–16]. Forces transmitted across these pathways have been demonstrated to elicit epigenetic alterations capable of directing cell identity processes including survival, differentiation, and cell cycle regulation in diverse cell types ranging from stem cells to specialized chondrocytes, tenocytes, alveolar cells and even cancer lines [17–21]. However, despite occupying mechanically demanding niches within musculoskeletal tissues, the mechano-adaptive strategies and epigenetic remodeling events regulating ligament cell function remain largely undefined.

Periodontal ligament (PDL) cells have emerged as invaluable cell sources for probing ligament regenerative mechanisms and cell biology [22–25]. Occupying a unique mechanical niche subjected to forces during mastication and swallowing, PDL cells likely harbor specialized tensional responsiveness [26–28]. While recent advances have begun unraveling how mechanical cues shape intracellular signaling and physiology in various contexts [29], interrogration of these events specifically within the PDL remain in its infancy. Here, we applied cyclic stretch as defined mechanical input to interrogate the timeline of mechanotransduction events in PDL cells, assessing impacts on focal adhesions, cytoskeleton, nuclear morphology, and epigenetics. These findings provide important frameworks for not only instructing tissue engineering approaches to regenerate functional ligament, but more fundamentally, decoding dynamic intracellular signaling pathways activated by mechanics in this clinically relevant cell population.

2. Material and methods

2.1. Human PDL cells

In this study, human periodontal ligament (PDL) cells from cementifying fibroma cell were used. The establishment of an immortalized human PDL cell line had been previously achieved through the transfection of human telomerase reverse transcriptase (hTERT) into human cementifying fibroma cells, resulting in a consistent PDL phenotype [30]. This PDL cell line's efficacy and suitability for PDL-related functions were validated in prior studies [31]. These cell lines are referred to as immortalized human PDL cells. The PDL cells were cultured in Dulbecco's modified Eagle's medium (DMEM, LM001-05, Welgene, Gyeongsan, Korea) supplemented with 10 % fetal bovine serum (FBS, 35-015-CV, Corning Inc., Corning, NY, USA), 1 % MEM non-essential amino acids solution (MEM NEAA, 11140050, Gibco™, Thermo Fisher Scientific, Inc., Waltham, MA, USA), 1 % GlutaMAX™ supplement (3505006, Gibco™), 1 % Penicillin-Streptomycin (15140-163, Gibco™) and 0.2 % 2-Mercaptoethanol (21985023, Gibco™) at 37 °C in a 5 % CO_2 incubator. The medium was changed every 2 days throughout the experiment.

2.2. Application of cyclic tensile stress to PDL cells

Cyclical tensile force was applied to PDL cells with a Flexcell FX-5000 Strain-Unit (Flexcell International Corporation, Burlington, NC, USA). Before seeding, PDL cells cultured in serum-free medium for 24 h to synchronize the cell cycle of PDL cells. PDL cells were seeded at a density of 6×10^4 cells/well in 6-well, 35-mm flexible bottomed uniflex plates culture plates (UF-4001C, Flexcell International Corporation). After 1 h incubation, the cells in the experimental groups were subjected to cyclic stretch of 10 % deformation at 6 cycles/min (10 % elongation, 4 s elongation and 6 s relaxation) for 2 h using a Flexcell Tension System (FX-5000, Flexcell International Corporation). On the other hand, cells in the control groups were cultured for 2 h without cyclic stretch (Fig. 1A). All cells were maintained in a humidified atmosphere containing 5 % CO_2. To observe cellular responses to mechanical force, inhibitors were applied 30 min before cyclic stretch. The histone acetyltransferase inhibitor C646 (10 μM; #4200, Tocris Bioscience, Bristol, UK) was used to inhibit p300/CREB-binding protein and anacardic acid (40 μM; a.a.; #A7236, Sigma-Aldrich, St. Louis, MO, USA) for noncompetitive PCAF/p300 inhibition. The cytoskeleton inhibitors used were blebbistatin (100 μM; #1760, Tocris Bioscience) to inhibit myosin II, nocodazole (0.5 μM; #M1404, Sigma-Aldrich) to inhibit microtubules and cytochalasin D (0.5 μM; Cyto D; #1233, Tocris Bioscience) to inhibit actin polymerization. As the inhibitors were dissolved in dimethyl sulfoxide (DMSO; #D8418, Sigma-Aldrich), DMSO was used as the control.

2.3. Immunocytochemistry (ICC)

PDL cells were fixed after 2 h of cyclic stretch on 4 % paraformaldehyde for 15 min at RT. After fixation, the cells were washed thrice in phosphate buffered saline (PBS) and permeabilized with 0.2 % Triton X-100 (Sigma-Aldrich) for 10 min, blocked with 1 % Bovine serum albumin Fraction (BSA, SM-BOV-100, Geneall, Seoul, Korea) for 1 h, incubated with primary antibodies (diluted in 1 % BSA) at 4 °C overnight. The following primary antibodies were used: Rabbit Anti-acetyl-Histone H3 Antibody (H3Ace; #06-599, Sigma-Aldrich), Mouse Histone H3 (Trimethyl Lys9) Antibody (H3K9me3; # NBP1-30141, Novus Biological, Centennial, CO), Rabbit Beta tubulin Antibody (#2146s, Cell signaling Technology, Danvers, MA, USA), Mouse Monoclonal Anti-Tubulin Acetylated Antibody (#T6793, Sigma-Aldrich), Mouse Lamin A/C (4C11) Antibody (#4777s, Cell Signaling Technology), Rabbit Phospho-Myosin Light Chain 2 (Ser19) Antibody (p-MLC2; #3671L, Cell Signaling Technology), Rabbit Vinculin Antibody (#ab129002, Abcam plc, Cambridge, UK), Mouse focal adhesion kinases (FAK) (D-1) Antibody (#sc-271126, SantaCruz Biotechnology Inc., Dallas, TX, USA). After the primary antibody incubation, cells were

washed with PBS and treated with the secondary antibody diluted in 1 % BSA at room temperature for 90 min. The following secondary antibodies were used: Fluorescein (FITC) AffiniPure Donkey Anti-Rabbit IgG (H + L) (#711-095-152, Jackson ImmunoResearch, West Grove, PA, USA). FITC AffiniPure Donkey Anti-Mouse IgG (H + L) (#715-095-150, Jackson ImmunoResearch), Rhodamine (TRITC) AffiniPure Donkey Anti-Rabbit IgG (H + L) (#711-025-152, Jackson ImmunoResearch, West Grove, PA), TRITC AffiniPure Donkey Anti-Mouse IgG (H + L) (#715-025-150, Jackson ImmunoResearch), Goat Anti-Mouse IgG Antibody (#bs-0296g-bf647, Bioss Antibodies, Woburn, MA). Following PBS washing, f-actin was stained by using Alexa Fluor™ 546-conjugated phalloidin (#A22283, Invitrogen, Thermo-Fisher Scientific, Waltham, MA, USA) and nuclei were stained with 4′,6-diamidino-2-phenylindole dihydrochloride (DAPI; #D9542; Sigma-Aldrich) diluted in PBS. Randomly selected stained cells were observed under a fluorescent microscope (IX71, Olympus, Tokyo, Japan) or a confocal microscope microscope (Nikon AX/AX R Confocal, Tokyo, Japan). Quantitative analysis of Lamin A/C profile using NIS-element software (Nikon). Intensity of Lamin A/C according to the distance of each group was measured.

2.4. QuantSeq mRNA 3′ sequencing analysis

2.4.1. RNA isolation

Total RNA was isolated using Trizol reagent (Invitrogen). RNA quality was assessed by Agilent 2100 bioanalyzer using the RNA 6000 Nano Chip (Agilent Technologies, Amstelveen, The Netherlands), and RNA quantification was performed using ND-2000 Spectrophotometer (Thermofisher Inc).

2.4.2. Library preparation and sequencing

For control and test RNAs, the construction of library was performed using QuantSeq 3′mRNA-Seq Library Prep Kit (Lexogen, Inc., Greenland, NH, USA) according to the manufacturer's instructions. In brief, each total RNA were prepared and an oligo-dT primer containing an Illumina-compatible sequence at its 5′end was hybridized to the RNA and reverse transcription was performed. After degradation of the RNA template, second strand synthesis was initiated by a random primer containing an Illumina-compatible linker sequence at its 5′end. The double-stranded library was purified by using magnetic beads to remove all reaction components. The library was amplified to add the complete adapter sequences required for cluster generation. The finished library is purified from PCR components. High-throughput sequencing was performed as single-end 75 sequencing using Next Seq 500 (Illumina, Inc., San Diego, CA, USA).

2.4.3. Data analysis

QuantSeq 3′mRNA-Seq reads were aligned using Bowtie2 [32]. Bowtie2 indices were either generated from genome assembly sequence or the representative transcript sequences for aligning to the genome and transcriptome. The alignment file was used for assembling transcripts, estimating their abundances and detecting differential expression of genes. Differentially expressed gene were determined based on counts from unique and multiple alignments using coverage in Bedtools [33]. The RC (Read Count) data were processed based on TMM + CPM normalization method using EdgeR within R (R development Core Team, 2020) using Bioconductor [34]. Gene classification was based on searches done by DAVID (http://david.abcc.ncifcrf.gov/) and Medline databases (http://www.ncbi.nlm.nih.gov/).Data mining and graphic visualization were performed using ExDEGA (Ebiogen Inc., Seoul, Korea).

2.5. Evaluation of cellular defense mechanisms

We evaluated the defense mechanisms of PDL cells by treating them with *N*-(3-Oxododecanoyl)-L-homoserine lactone (Bacterial quorum sensing signal molecules, 6548, TOCRIS, Bristol, UK) and Hydrogen peroxide solution (H_2O_2, H1009, Sigma-Aldrich). To investigate the defense response upon stretch, we treated the reagents together when using the Flexcell Tension System. PDL cells were seeded at the same density as the application of cyclic tensile stress, and after 1 h of incubation, the cells were replaced with medium supplemented with quorum sensing signal molecule (QS) and H_2O_2 to perform stretching for 2 h. Cells in the control group were incubated in the incubator for 2 h without stretching. After 2 h, the cells were washed with phosphate buffer saline (PBS, BPB-9121-004LR, T&I, Seoul, Republic of Korea) and replaced with growth medium to see the response of the cells to QS and H_2O_2. The Cell Counting Kit-8 (CCK-8, CK04-20, Dojindo, Kumamoto, Japan) assay was used to assess the viability of PDL cells. The CCK-8 assay measures the activity of mitochondrial dehydrogenase in living cells, which is a marker of cell viability. After 24 h of incubation, the samples were washed with PBS and then incubated for 4 h at 37 °C in 2 ml of culture medium with 200 μl of CCK-8 added to each well. The optical density value was measured at 450 nm absorbance using a microplate reader (Scientific Varioskan LUX Multimode Microplate Reader, Thermo Fisher Scientific).

Table 1
Primers sequence.

Genes	Forward primers (5′-3′)	Reverse primers (5′-3′)
GAPDH	GGAGCGAGATCCCTCCAAAAT	GGCTGTTGTGCATACTTCTCAT
FAK	CCAGGATCCAAAATGTGGCG	GCTTCTAGCTCTCCTCTTCC
Vinculin	CTTGTGCACCCTCTATCCCA	GGAGCCAAGGAAAGAGAAAC
M-CSF1	ATGAGACACCTCTCCAGTTGC	GGCTTGGTCACCACATCTTG
JUNB	GGACACGCCTTCTGAACG	CGGAGTCCAGTGTGGTTTG
MMP9	GCATAAGGACGACGTGAATGGC	CGGTGTGGTGGTGGTTGGAG
RUNX2	GCTTCATTCGCCTCACAAAC	GTAGTGACCTGCGGAGATTAA
Col1	AAGTCTTCTGCAACATGGAG	TACTCGAACTGGAATCCATC
OPN	CATACAAGGCCATCCCCGTT	TGGGTTTCAGCACTCTGGTC
α-SMA	GTTCCGCTCCTCTCTCCAAC	GTGCGGACAGGAATTGAAGC
c-fos	GCCTCTCTTACTACCACTCACC	AGATGGCAGTGACCGTGGGAAT

2.6. Quantitative real time-polymerase chain reaction (qRT-PCR)

The gene expression was evaluated by real-time polymerase chain reaction (qRT-PCR). Total RNA was extracted with Ribospin™ II (Geneall) and reverse-transcribed using AccuPower® RT PreMix (Bioneer, Korea). qRT-PCR was performed using a Fast SYBR green master mix (QT605-05, Meridian Bioscience, Cincinnati, OH, USA) and StepOneTM (Applied Biosystem, Waltham, MA, USA). Relative gene expression levels were quantified using the ΔΔ Ct method and normalized to an endogenous housekeeping gene, glyceraldehyde 3-phosphate dehydrogenase (GAPDH). The sequence of primers was described in Table 1.

2.7. In vivo model of hypo-occlusion induced by tooth extraction

The animal study was approved by the Institutional Animal Care and Use Committee of Dankook university. Sprague Dawley rats, 6-week-old, male (n = 3), from company (DBL, Eumseong, Korea) were used. During the experimental period, a 12 h light and 12 h dark cycle was maintained. The rats had an adaptation period for 7 days before the experiment.

Under ketamine/Rumpun anesthesia, right upper 1st molar of rat was extracted for inducing hypo-occlusion force. After 4 weeks, the animals were sacrificed by CO_2 overdose. The maxillary region was fixed for one week at room temperature in 10 % neutral buffered formalin, followed by decalcification in 0.5 M EDTA solution for two weeks at 37 °C. Subsequently, it was embedded in paraffin blocks, and staining with Hematoxylin and Eosin (H&E), Masson's Trichrome (MT) were performed.

For measuring nuclear aspect ratio, we observed the nuclei of PDL

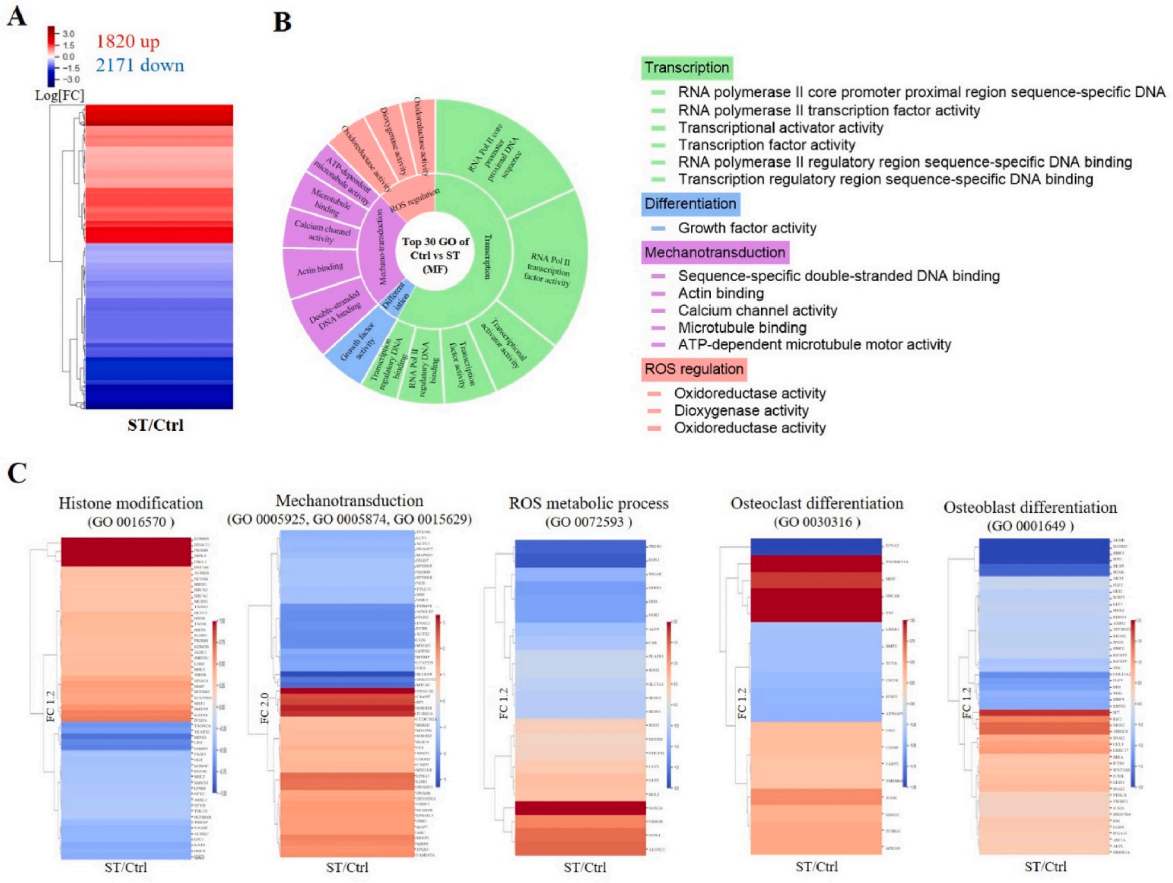

Fig. 2. Transcriptome analysis revealing signaling pathways activated by stretch in periodontal ligament cells. (**A**) Heat-map of distance-based clustering analysis of global transcriptional changes, showing a total of 3991 regions between ctrl and stretch (45.6 % up versus 54.4 % down). (**B**) Top 30 enriched Gene ontology (GO) analysis of molecular functions associated with the upregulated differentially accessible regions in ST. Enrichment in transcription pathways, including RNA polymerase II transcription factor activity, Transcriptional activator activity, etc., and pathways related to mechanotransduction (Sequence-specific double-stranded DNA binding, Actin binding, Microtubule binding, etc.) and differentiation, reactive oxygen species (ROS) regulation conditions were also identified. (**C**) Heat-map analysis of GO terms related to histone modification, mechanotransduction, ROS metabolic process, osteoclast differentiation, osteoblast differentiation. Ctrl; control group, without stretch ST; stretch induced group.

cells in the middle 1/3 region, using Digimizer software (MedCalc Software Ltd, Ostend, Belgium). The short axis and long axis lengths of the nuclei were measured, and the nuclear aspect ratio was calculated by dividing the short axis length by the long axis length. Also, elongation factor was calculated by dividing the long axis by the short axis. Additionally, the angle between the tooth long axis and cell of periodontal ligament was also measured.

Immunohistochemistry (IHC) protocols included heat-induced epitope retrieval. Tissue sections were immersed in 0.1 M citrate buffer at pH 6 and heated to 95 °C for 10 min. This was followed by rehydrating the sections with three washes using PBS containing 0.1 % Tween as the wash buffer. The IHC staining itself was then carried out following the manufacturer's recommended procedures using the EnVision HRP detection kit (k4006, Dako) and H3Ace antibody (1:500, #06-599, Sigma-Aldrich). For quantification of IHC staining, image J with IHC toolbox plugin was used.

2.8. Statistical analysis

All experiments were performed three biological replications to confirm reproducibility, and the representative results among them were presented. Statistical tests were performed by GraphPad Prism 9.5.1. Normally distributed data were analyzed by one-way ANOVA with Tukey's post hoc test or unpaired *t*-test as indicated in each figure legend. Values of $p < 0.05$ were considered statistically significant. The error bars of all bar graphs were indicated as standard error of the mean (SEM).

3. Results & discussion

3.1. Stretch modifies the PDL cells' morphology and stimulates chromatin remodeling

To impose defined mechanical stimulation *in vitro*, based on the equipment and materials previously established in our laboratory, to understand the prominent effects, Flexcell tension culture plates were utilized for applying cyclic uniaxial stretch (4 s rest after 6 s strain) to PDL cells [19]. Following cyclic tensile loading, stretched PDLs exhibited upregulated expression of filamentous actin versus static controls across all timepoints examined. Furthermore, while unstrained cultures retained rounded or randomly-oriented morphologies, PDLs subjected to 1-6 h of cyclic stretch underwent conspicuous reorganization, realigning cell bodies perpendicular rather than parallel to the axis of applied strain. This tension-guided rearrangement into regular orientations perpendicular to the direction of elongation signifies that PDL cells actively remodel their cytoskeleton in response to mechanical cues [35]. To quantify realignment, the angle between the cell's major axis and strain vector perpendicular was measured. While static PDLs exhibited variable 0-180° orientations, stretched cells converged between 80 and 100°, confirming significant perpendicular reorientation. This

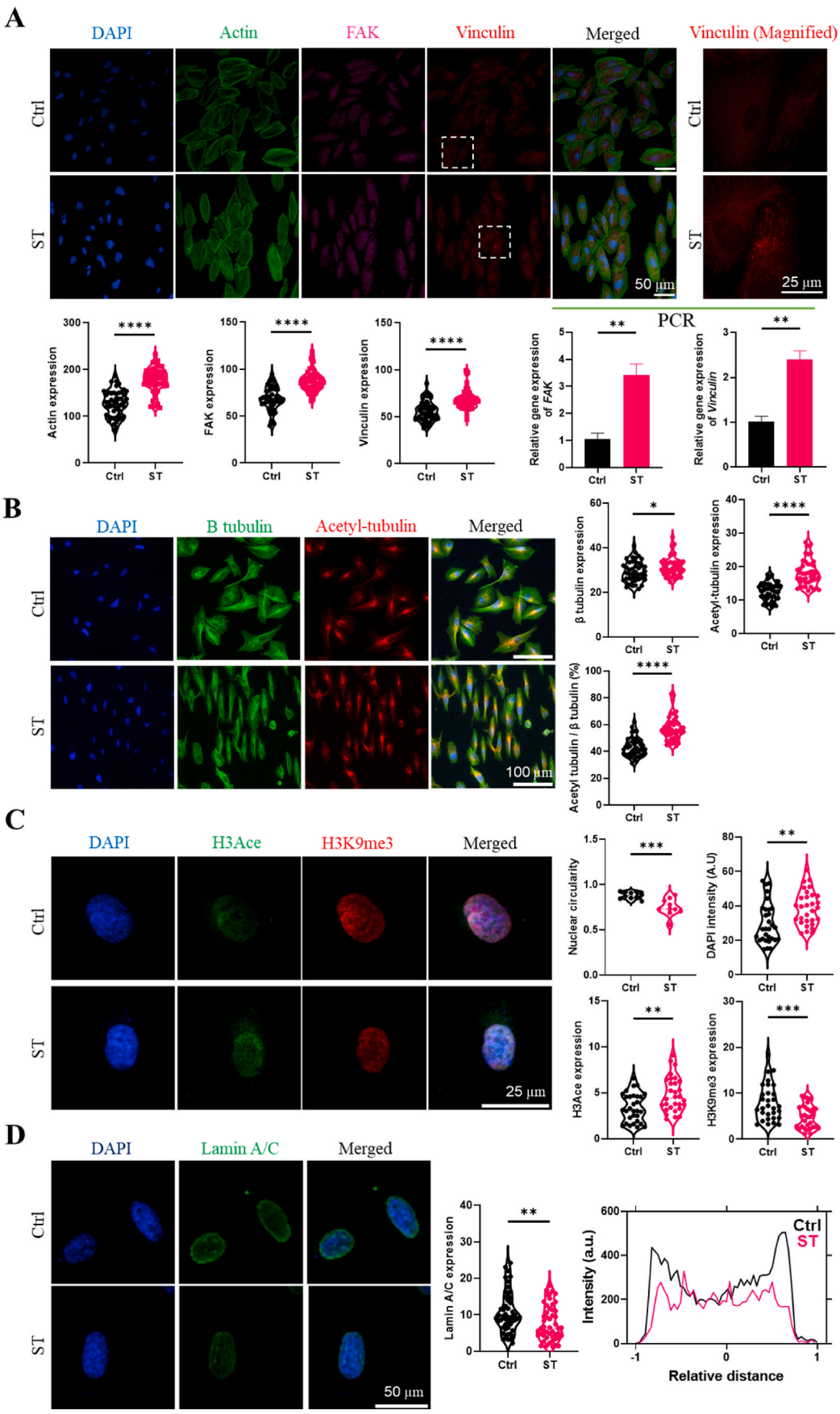

(caption on next page)

Fig. 3. Dynamic changes in focal adhesions, tubulin, histone modifications (H3Ace and H3K9me3), and lamin A/C in response to mechanical stretch in periodontal ligament cells. (A) Immunostaining images of focal adhesion kinase (FAK) and vinculin in Ctrl and ST, showing an increase in actin, FAK, and vinculin in ST. Triplicate biological experiments were performed and representative data from 50 cells were depicted. And quantitative RT-PCR analysis of mRNA levels for focal adhesion (FAK, vinculin), showing upregulated gene expression of FAK and vinculin in ST. Cells were cultured in growth medium for 1 day. (**B**) Immunofluorescence imaging of the expression of intracellular β tubulin (green) and acetylated tubulin (red) in Ctrl and ST. Quantitative analysis of the expression of β tubulin, acetylated tubulin, and acetyl tubulin/β tubulin (%) confirmed that the expression levels were significantly higher in ST compared to ctrl. Triplicate biological experiments were performed and representative data from 45 cells were depicted. (**C**) Immunofluorescence images of DAPI-stained nucleus and H3Ace (green) and H3K9me3 (red). Quantitative analysis of DAPI and H3Ace and H3K9me3 expression indicated increased expression of DAPI and H3Ace and decreased expression of H3K9me3 in ST compared to Ctrl. Triplicate biological experiments were performed and representative data from 30 cells were depicted. (**D**) Immunofluorescence imaging of Lamin A/C. Quantitative analysis of Lamin A/C expression showed decreased expression of Lamin A/C in ST. Intensity profile analysis of Lamin A/C in the nuclei of Ctrl and ST indicated that Lamin A/C was localized to the nuclear edge in Ctrl than in ST. Triplicate biological experiments were performed and representative data from 50 cells were depicted. $^{*}P < 0.05$, $^{**}P < 0.005$, $^{***}P < 0.0005$, or $^{****}P < 0.0001$, unpaired *t*-test. In the line graph, black indicates Lamin A/C intensity according to the distance from Ctrl and red indicates Lamin A/C intensity according to the distance from ST. All bar plots show mean value ± SEM. Ctrl; control group, without stretch ST; stretch induced group. (For interpretation of the references to color in this figure legend, the reader is referred to the Web version of this article.)

tension-guided transition from random to highly aligned distributions means that cyclic stretch elicits distinct cytoskeletal remodeling and repositioning of cell bodies as a form of structural mechano-response [36]. Such tension-guided rearrangement from irregular to highly aligned morphology indicates active cytoskeletal remodeling, enabling PDLs to dynamically adapt to mechanical forces. Through structural rearrangement, cells likely optimize mechano-sensing and downstream transformation of physical cues. Ultimately, these findings spotlight the remarkable capability of periodontal ligaments to detect and respond to mechanical loading through self-reorganization. Achieving aligned cellular orientations is critical in maintaining tissue integrity and function within the demanding mechanical environment of the periodontium [37,38]. This capacity to actively remodel cytoskeletal architecture represents an essential adaptive response enabling effective force transmission from the tooth to the surrounding alveolar bone, critical for preserving mechanical stability and functional integrity of the periodontal tissue.

Histone acetylation represents a vital epigenetic modification capable of extensively reshaping downstream gene expression programs. Acetylation of histone proteins neutralizes the positive charge of lysine residues, relaxing higher-order chromatin structure to render DNA more permissible and accessible to transcription factors and regulatory proteins [39]. This relaxation of chromatin architecture facilitates transcriptional activation, enabling tight and dynamic regulation over expression of specific gene subsets along with diverse nuclear processes integral to modulating cell function, differentiation trajectories, and stimulus-adaptation responses [40]. Indeed, under applied mechanical stress, the nucleus and chromatin dynamically remodel their intrinsic physical properties to safeguard genomic integrity, ultimately governing downstream functional responses [41]. Therefore, to assess impacts of cyclic stretch on chromatin remodeling dynamics, H3Ace immunofluorescence was conducted over a 0-6 h timecourse as a marker of transcriptional accessibility (Fig. 1C). Quantification verified cyclic tension elicited a progressive upregulation in H3Ace and DAPI intensity over basal unstretched levels, peaking at 2 h before declining. This stretch duration eliciting maximal chromatin loosening was therefore selected for subsequent mechanistic analyses. These quantifications verify cyclic substrate deformation promotes chromatin relaxation in periodontal ligaments, as evidenced by enhanced acetylation-mediated transcriptional accessibility. Through modulating H3Ace status, cyclic stretch may reshape chromatin organization to influence transcriptional programs underlying PDL mechanotransduction. While these data verify stretch-induced chromatin loosening potententiates gene accessibility, the precise transcriptional networks and signaling cascades affected by altered H3Ace signatures remain to be fully elucidated. Further interrogation is vital to decode specific gene subsets and post-translational modulations involved in transducing mechanical signals into functional cell fates and behaviors.

Additionally, levels of p-MLC2 were examined to probe activation of myosin contractility pathways governing actomyosin cytoskeletal dynamics, structural remodeling, and motile responses (Fig. 1D) [42]. Quantification revealed cyclic stretch elicited decreased p-MLC2 expression after 2 h, indicating mechanical tension transiently suppresses actomyosin contractility. This temporary reduction in actin-myosin crosslinking could promote architectural rearrangement of the cytoskeleton, providing a structural foundation for observed stretch-induced cell reorientation and morphological adaptations [43]. Ultimately, this mechanically-triggered suppression of cytoskeletal contractility pathways represents an adaptive response promoting cellular rearrangement essential for preserving functional stability and tissue homeostasis within the demanding mechanical environment of periodontal tissue.

3.2. *QuantSeq 3′ mRNA-sequencing to determine functions and signaling pathways activated by stretch*

To elucidate transcriptional networks altered by tensional loading, RNA-sequencing based transcriptomic profiling was conducted with subsequent bioinformatic analyses. Fig. 2A shows the distance-based clustering analysis of global transcriptional changes in the ST/Ctrl group. 1820 up-regulated genes and 2171 down-regulated genes in ST/Ctrl are shown, which were used for Gene Ontology (GO) analysis by DAVID. This resulted in the top 30 enriched GO terms categorized into biological process (BP), molecular function (MF), and cellular component (CC) analyses; mainly transcription (RNA polymerase II core promoter proximal region sequence-specific DNA, RNA polymerase II transcription factor activity, Transcriptional activator activity, Transcription factor activity, RNA polymerase II regulatory region sequence-specific DNA binding), differentiation (Growth factor activity), mechanotransduction (Sequence-specific double-stranded DNA binding, Actin binding, calcium channel activity, Microtubule binding, ATP-dependent microtubule motor activity), and ROS regulation (Oxidoreductase activity, Dioxygenase activity, Oxidoreductase activity) conditions were found to be enriched (Fig. 2B, Supplementary Fig. 1 and Supplementary Fig. 2). Individual heat maps from each GO term detected by DAVID analysis also displayed genes that were differentially expressed after stretch; especially histone modification (*HDAC11*, *PRDM9*, *HIPK4*, *FBLL1*, etc.), mechanotransduction (*ACTA*, tubule, etc.), osteoclast differentiation (*TNF*, *OSCAR*, *MITF*, *JUNB*, etc.), osteoblast differentiation (*SP7*, *AMELX*, *CCL3*, *LRRC17*, etc.), and ROS metabolic process (*NOXA1*, *NRROS*, *NOX4*, *ALOX12*, etc.) were significantly upregulated in ST compared to ctrl (Fig. 2C). Combined together, it was unveiled that global transcriptional change occurred after stretch in PDL cells, supporting change in epigenetic modification (H3Ace) and mechanotransduction signaling (actin and tubules), as well as suggesting other biologic processes related to lineage specification and ROS metabolism. In existing literature, stretch force was known to have a close association with osteoblast formation. The research by Wu et al. suggested that the pathway activated by applying stretch force to PDL could stimulate the Hippo pathway and act as a positive regulator in bone formation [44]. On the other hand, osteoclastic genes were known to be primarily expressed in environments where compressive force was applied [45]. In

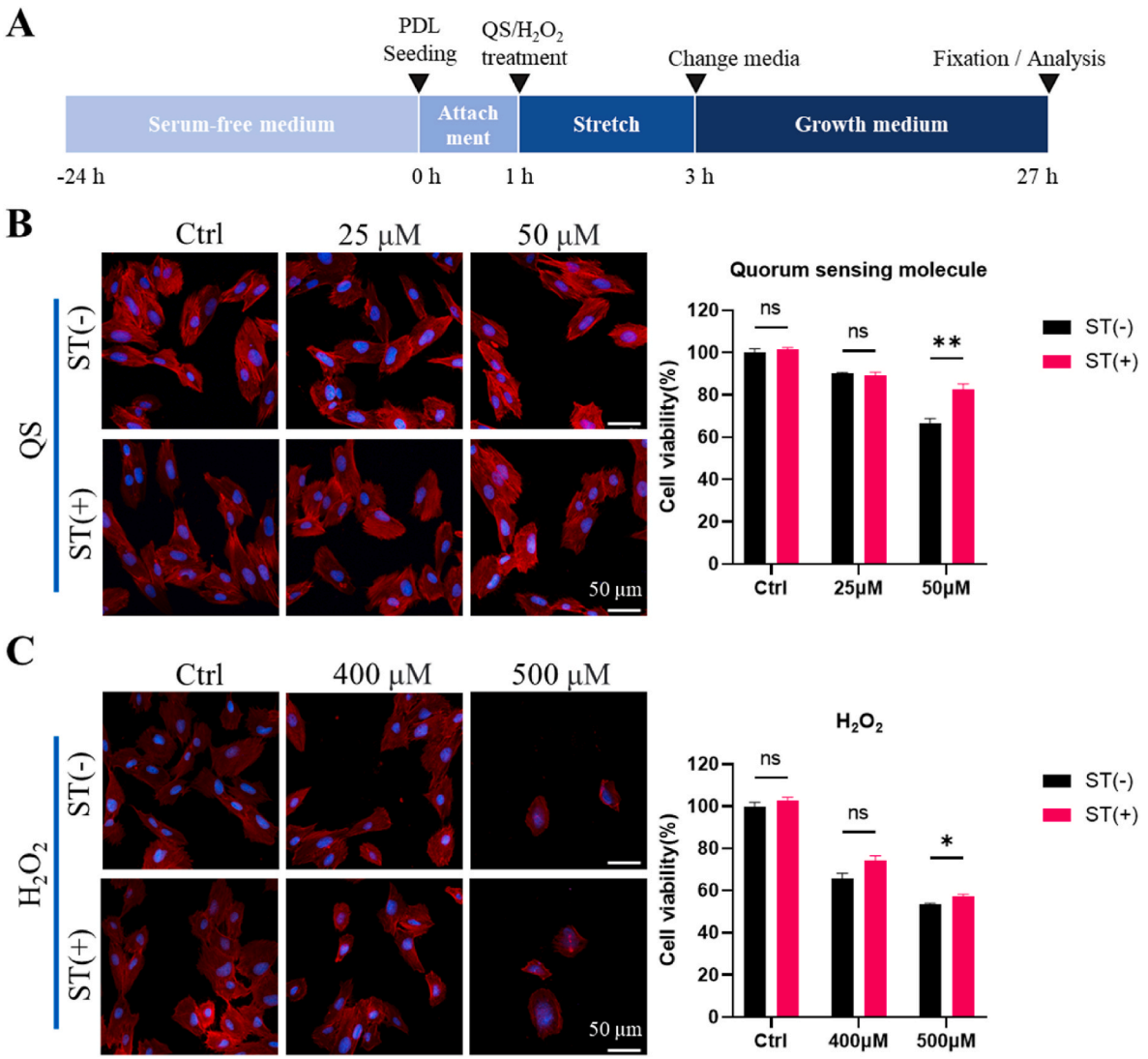

Fig. 4. Effects of stretching induced euchromatin structure enhances the cell survival of PDL cells against the quorum-sensing signaling molecule, C12-HSL, or H_2O_2 attack. (**A**) Culture timetable and conditions for chemical induction. Cells were cultured in serum-free medium for 24 h and then seeded and attached for 1 h. The cells were then stretched for 2 h simultaneously with QS (quorum sensing signaling molecule) or H_2O_2 treatment. The cells were then cultured in growth medium for an additional 24 h and analyzed. (**B**) Cell survival study by QS treatment, confirmed the cell morphology and cell viability of the stretch effect. CCK-8 assay revealed significantly higher cell viability in ST (+) compared to ST (−) at a concentration of 50 μM (n = 3). Red; actin, Blue; DAPI. (**C**) Cell survival study through treat H_2O_2, confirming cell morphology and cell viability of the stretch effects. CCK-8 assay showed significantly higher cell viability in ST (+) versus ST (−) at a concentration of 500 μM (n = 3). Red; actin, Blue; DAPI. $^*P < 0.05$, $^{**}P < 0.005$, ns; non-significant, unpaired *t*-test. All bar plots show mean value ± SEM. Ctrl; control group, without stretch ST; stretch induced group. (For interpretation of the references to color in this figure legend, the reader is referred to the Web version of this article.)

this experiment, no additives inducing osteogenesis were added to the media; only the stretch-induced condition was applied. However, various changes in gene expression occurred. This could be attributed to the influence of epigenetics, inducing dramatic changes [19].

3.3. Mechanical stretch leads to dynamic modifications of focal adhesion, histone modifications (H3Ace and H3K9me3), lamin A/C, and tubulin in PDL cells

Here, we interrogated impacts of cyclic tensile loading on focal adhesions, tubulin cytoskeletal networks, histone modification markers (H3Ace and H3K9me3), and the nuclear envelope component lamin A/C within PDL cells (Fig. 3). Focal adhesions comprise intricate clusters of structural and signaling proteins capable of actively mediating dynamic mechanical linkages between the intracellular actin cytoskeleton and extracellular matrix niche [10]. Focal adhesions perform vital mechanotransductive functions, dynamically relaying biophysical cues from the extracellular matrix to modulate integral cellular processes encompassing migration, proliferation, differentiation, and survival [46,47]. Increased formation of focal adhesions in PDL cells generally leads to enhanced cell adhesion, migration, and mechanical deformation [48]. Therefore, to verify the results of focal adhesion formation in PDL cells upon stretch stimulation, we examined the expression levels of focal adhesion kinase (FAK) and vinculin, which are involved in focal adhesion (Fig. 3A). As a result, we observed that FAK, which is involved in signal transduction pathways related to cell adhesion and migration, was significantly increased in expression in the stretch group. Furthermore, vinculin, a cytoskeletal protein that connects integrins and actin, was upregulated in the stretch group. Furthermore, magnified vinculin imaging revealed enhanced vinculin dot expression upon stretching. Subsequently, to examine stretch-induced cellular responses in PDL cells, gene expression analysis was performed following additional 24 h culture post 2 h stretching. Under these conditions, elevated FAK and vinculin levels were observed in stretched cells after 24 h growth

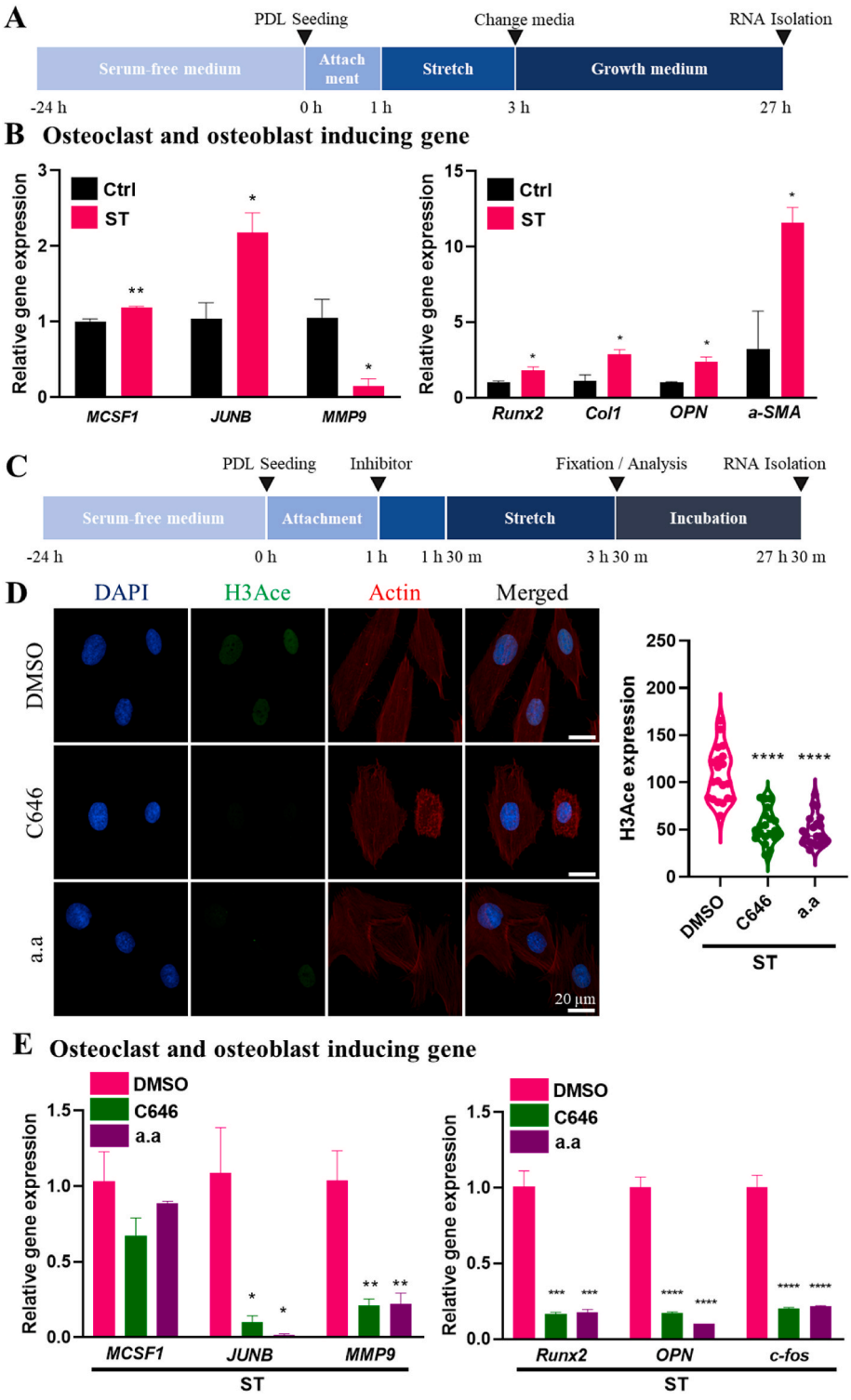

Fig. 5. Stretch-induced regulation of osteoclast and osteoblast differentiation. (**A**) Culture timetable and conditions. Cells were cultured in serum-free medium for 24 h and then seeded and attached for 1 h. Stretch was then applied for 2 h, and cells were cultured for an additional 24 h in growth medium without lineage differentiation biochemical factors. (**B**) Quantitative RT-PCR analysis of mRNA levels for osteoclast differentiation genes (*MCSF1*, *JUNB*, *MMP9*) and osteoblast differentiation genes (*Runx2, Col 1*, *OPN*, and *α-SMA*). ST cues upregulated significantly *MCSF1* and *JUNB* and downregulated significantly *MMP9*. Also ST cues upregulated significantly *Runx2, Col 1*, *OPN*, and *α-SMA*. (n = 3) $^{*}P < 0.05$ or $^{**}P < 0.005$, unpaired *t*-test. (**C**) Culture timetable and conditions of inhibitor study. **(D)** Study on histone acetyltransferase inhibitors to identify the correlation between H3Ace and osteoclast and osteoblast genes (C646 and anacardic acid (a.a)). Inhibition of H3Ace was observed when inhibitors (C646 and anacardic acid (a.a)) were treated. All groups were compared to DMSO. Triplicate biological experiments were performed and representative data from 20 cells were depicted. **(E)** Quantitative RT-PCR analysis of mRNA levels for osteoclast differentiation genes (*MCSF1*, *JUNB*, *MMP9*) and osteoblast differentiation genes (*Runx2, OPN*, and *c-fos*). When H3Ace was inhibited, gene expression decreased except for MCSF1. (n = 3) $^{*}P < 0.05$, $^{**}P < 0.005$, $^{***}P < 0.0005$, or $^{****}P < 0.0001$, ns; non-significant, one-way ANOVA with Tukey's post hoc test. All bar plots show mean value ± SEM. Ctrl; Control group, without stretch ST; stretch induced.

medium incubation compared to static controls. The upregulation of these focal adhesion regulators implies that stretching may promote focal adhesion assembly and maturation in PDL cells.

β-Tubulin is a structural constituent of microtubules, cytoskeletal filaments critical for regulating cell morphology, intracellular trafficking, and mitosis [49]. Tubulin acetylation denotes post-translational modifications implicated in modulating microtubule stability and dynamics [50]. Assessing tubulin expression and acetylation in response to mechanical stretch illuminates stretch-mediated control of microtubule-dependent functions such as cell motility, differentiation, mechanotransduction, and cytoskeletal reorganization. We detected increased levels of both β-tubulin and acetylated tubulin upon mechanical stretching, confirming stretch-induced upmodulation of their expression (Fig. 3B). Furthermore, stretched cells exhibited a higher β-tubulin to acetylated tubulin ratio, implying mechanical stretch may augment tubulin polymerization and acetylation, thus stimulating microtubule dynamics and cytoskeletal remodeling [51].

H3Ace and H3K9me3 denote epigenetic histone marks that regulate chromatin configuration and transcriptional activity [41]. By modulating DNA availability to the transcription apparatus, histone marks govern diverse cellular processes encompassing proliferation, differentiation and responses to exogenous cues [52]. To examine the dynamic modulations on gene expression and chromatin remodeling under mechanical stretch in PDL cells, we evaluated the expression levels of H3Ace and H3K9me3 (Fig. 3C). The results showed an increase in DAPI intensity along with changes in nuclear circularity in the stretch group. While the nuclei in the control group were circular, the nuclei in the stretch group appeared elongated. In addition, the expression of H3Ace increased, while the expression of H3K9me3 decreased in response to mechanical stretch. These results provide evidence that mechanical stretch leads to modifications in chromatin structure in PDL cells, increasing H3Ace and decreasing H3K9me3. These histone modifications suggest potential effects on chromatin structure and gene regulation as a reaction to mechanical stimulation.

Lamin A/C are the structural proteins in the nuclear lamina, the network of intermediate filaments that structurally supports the nuclear shape and integrity [53,54]. As nuclear scaffold proteins, lamin A/C coordinate chromatin organization, transcriptional control, and mechanical robustness of the nucleus [55]. Thus, we investigated lamin A/C expression upon mechanical stretch to provide insight into its effects on cellular processes including gene expression, mechanical modulation of nuclear structure, nuclear signaling, and mechanotransduction. We assessed the influence of mechanical stretch on the lamin A/C expression and observed a decrease in lamin A/C expression in the stretch group versus the control group (Fig. 3D). This decrease in lamin A/C expression suggests that mechanical stretch could influence the structural integrity of the nucleus, thereby affecting cellular functions associated with lamin A/C, including gene regulation and nuclear organization.

In summary, this finding provides cellular responses of PDL cells in response to mechanical stretch. An increase in focal adhesion proteins indicates an enhanced ability of PDL cells to respond to mechanical signals and adhere. Increases in β-tubulin, acetylated tubulin, and histone modifications suggests dynamic changes in cell cytoskeletal organization and chromatin structure. In addition, the reduction in lamin A/C expression suggests a potential remodeling in nuclear structure under mechanical stretch. By investigating specific molecules and cellular components, we provided a comprehensive understanding of the various cellular responses and adaptations that occur in PDL cells under mechanical stretch conditions. This study elucidates the complex mechanobiology of PDL cells, which provides a target for potential therapeutic approaches for periodontal tissue regeneration and tissue engineering.

3.4. Stretch protects periodontal ligament cells from external attack induced by QS/H_2O_2

In intact periodontal tissue, resident PDL cells persistently experience mechanical tension and accordingly maintain aligned orientations [56]. However, pathological conditions like periodontitis disrupt native tissue tension, leading PDL cells to lose aligned configurations and compromise defense mechanisms, thereby facilitating disease establishment [57,58]. We suggested that the gene transcription and activity of the PDL cells are altered by the stretch stimulus, affecting the cell survival. We have shown in Fig. 2 that H3Ace changed the chromatin structure to a relaxed euchromatin structure by stretch. Therefore, we expected that chromatin decondensation may have enhanced gene transcription and activity, thereby improving the cell's defense mechanisms against external attacks, and we checked whether it affected cell viability (Fig. 4). In this study, periodontal ligament cells were treated with QS and H_2O_2 in a stretched environment and cell viability was measured. We co-treated the QS and H_2O_2 at the time of stretch treatment, and then incubated the cells in growth medium for an additional 24 h to ensure proper effect. Cell viability was first measured at two different concentrations of QS, 25 μM and 50 μM. At 25 μM, no significant difference in cell viability was observed compared to the ST (−) group (Fig. 4a). Cells treated with 50 μM of QS showed increased viability compared to the ST (−) group. This indicates that QS had a beneficial effect on the viability of periodontal ligament cells in a stretch environment. Next, cell viability was measured in response to 400 μM and 500 μM of H_2O_2 (Fig. 4b). At 400 μM, no significant difference in cell viability was observed compared to the ST (−) group. However, at 500 μM, a significant difference in cell viability was observed. Cells treated with 500 μM H_2O_2 showed increased viability compared to the ST (−) group. This indicates that, similar to QS, H_2O_2 levels boosted stretched PDL cells viability, implying mechanical loading may augment cellular antioxidant defenses. Ko et al. have shown *in vivo* that PDLs express less of the chemokine CXCL14 in the presence of orthodontic or tensile forces, providing evidence that stretch forces may increase PDL defense [59]. These findings indicate stretch-induced hormesis, wherein moderate oxidative challenge elicits compensatory responses conferring resistance to higher intensities of that stimulus. Thus, periodic mechanical stress may bolster PDL cells antioxidant capacity.

3.5. Stretch promotes osteoclast and osteoblast differentiation

Heatmap analysis in Fig. 2 illustrated mechanical stretch-induced transcriptional activation of osteoclast and osteoblast differentiation pathways in PDL cells. To validate these findings, we conducted PCR analysis targeting key genes associated with osteoclast and osteoblast differentiation (Fig. 5). To examine the cellular responses triggered by stretching stimulation in PDL cells, following a 2 h stretching treatment, gene expression was investigated by an additional 24 h culture. In this process, cells were maintained for 24 h in growth medium without biochemical factors for lineage differentiation (Fig. 5A).

To assess osteoclast differentiation, we investigated the gene expression levels of *MCSF1*, *JUNB*, and *MMP9* (Fig. 5B left). *MCSF1*, encoding macrophage colony-stimulating factor 1, was significantly upregulated in stretched PDL cells. This suggests that mechanical stretch promoted the expression of *MCSF1*, a critical regulator of osteoclast differentiation. In addition, the upregulation of *JUNB*, a transcription factor involved in osteoclastogenesis, indicated a potential enhancement of osteoclast differentiation under stretch stimulation. *MMP9* is a proteolytic enzyme that is involved in extracellular matrix remodeling. Downregulation of *MMP9* may prevent osteoclasts from effectively degrading the surrounding matrix. At the same time, however, *MMP9* is associated with inflammation, indicating that it limits the inflammatory response. Then, to investigate the stimulation of osteoblast differentiation of PDL cells under stretch, we analyzed the expression levels of genes related to osteoblast differentiation: *RUNX2*, *COL1*, *OPN* and

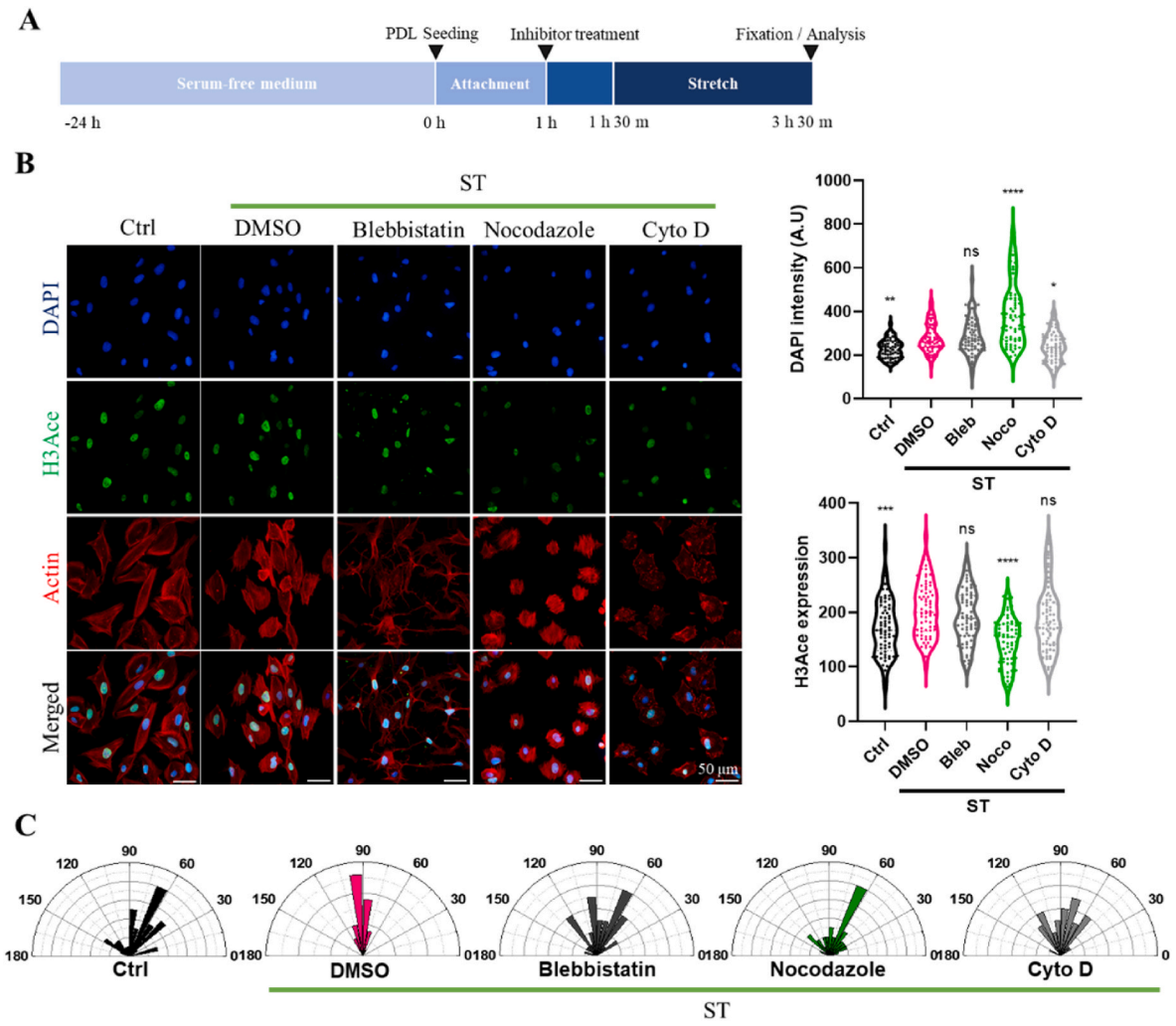

Fig. 6. Microtubules play a crucial role in mediating epigenetic modifications in periodontal ligament cells in response to stretching. (**A**) Culture timetable and condition for Inhibitor induction. Cells were cultured in serum-free medium for 24 h, and cells were seeded and attached for 1 h. Then, inhibitors were treated and incubated for an additional 30 min and stretch was applied for 2 h and analyzed. (**B**) Study on cell cytoskeleton inhibitors to identify key factors in the response of periodontal ligament cells to mechanical stretch (blebbistatin, nocodazole, and Cyto D). The ST nocodazole group showed decreased H3Ace expression compared to the ST DMSO group. All groups were compared to ST DMSO. Triplicate biological experiments were performed and representative data from 65 cells were depicted. $^{*}P < 0.05$, $^{**}P < 0.005$, $^{***}P < 0.0005$, or $^{****}P < 0.0001$, ns; non-significant, one-way ANOVA with Tukey's post hoc test. (**C**) Quantification of cell alignment, presented as rose plots of actin cytoskeleton orientation. All groups treated with the inhibitor lost cell alignment. Ctrl; control group, without stretch ST; stretch induced group.

α-SMA (Fig. 5B right).

Stretch stimulation significantly increased the expression of RUNX2, a key transcription factor essential for osteoblast differentiation and osteogenesis, indicating a positive influence of the stretch environment on osteoblast differentiation enhancement. Furthermore, the increase in COL1, which encodes collagen type 1, a major component of the bone extracellular matrix, suggested that the extracellular matrix is reorganized during osteoblast differentiation by stretch stimulation. The increased expression of *OPN* further supported the idea that the stretch environment positively affected osteoblast-related processes mediated by *OPN*. Additionally, the significant upregulation of myofibroblast activation marker α-SMA suggested that stretch stimulation impacted the activation of myofibroblasts, possibly playing a role in osteoblast differentiation [60–62]. Most genes responded to stretch in various ways, suggesting a complex role of stretch in osteoblast and osteoclast differentiation. These results lead to an improved understanding of the molecular mechanisms that regulate osteoblast and osteoclast differentiation in PDL cells under stretch stimulation.

To investigate the correlation between H3Ace and osteoclast and osteoblast genes, we inhibited histone acetyltransferase to see its effects on osteoclastic and osteoblactic genes (Fig. 5C). When we treated cells with C646, an inhibitor of histone acetyltransferase, and anarcadic acid (a.a) and checked the expression of H3Ace, we confirmed decreased expression of H3Ace even under Stretch conditions (Fig. 5D). When we checked changes in gene expression related to osteoblast and osteoclast differentiation under conditions of histone acetyltransferase inhibitor treatment, the inhibitor significantly decreased expression levels of osteoclast-related genes (*JUNB*, *MMP-9*) and osteoblast-related genes *RUNX2*, *OPN*, and *c-fos*. However, no change was observed in *MCSF1* (Fig. 5E). These results suggest that histone acetylation affects osteoclast and osteoblast genes expression.

3.6. The mediation of epigenetic modifications in periodontal ligament cells in response to stretch is driven by the crucial involvement of microtubules

To elucidate key regulators of the periodontal ligament cell response to mechanical stretch, we performed a cytoskeleton inhibitor study. Specifically, cells were pretreated with inhibitors prior to stretch application to delineate stretch-induced signaling cascades (Fig. 6A).

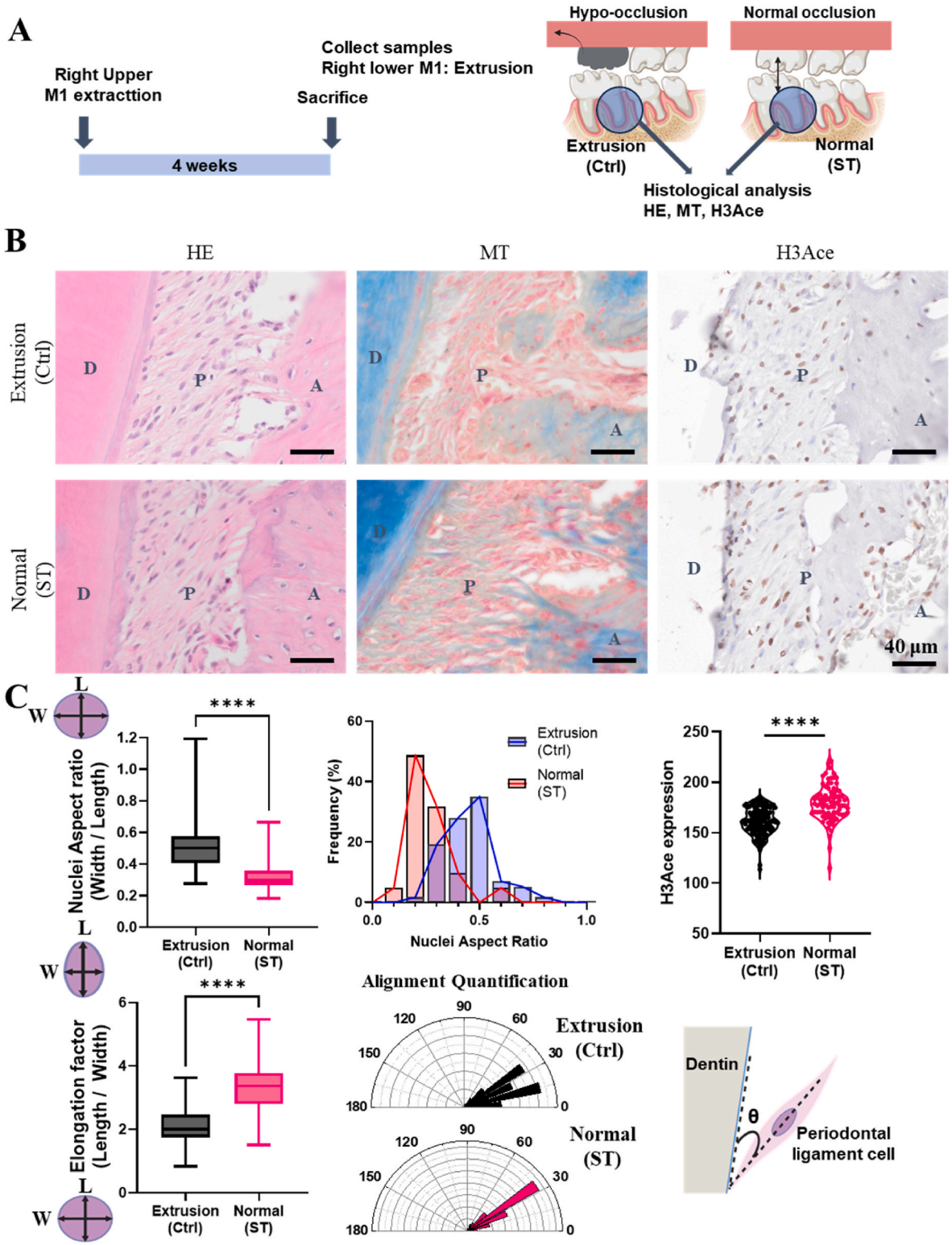

Fig. 7. Stretch force influenced the morphology and epigenetics of rat periodontal ligament cells. (**A**) Schematic image and timetable of *in-vivo* model of hypo-occlusion induced by tooth extraction. The natural periodontal ligament of normal (ST) group was in a constant stretched state due to continuous occlusal forces. To eliminate these forces, opposing teeth were extracted to induce extrusion that refers to the control group (Ctrl) in *in vitro* experiments (n = 3). (**B**) Representative hematoxylin and eosin (HE), Masson's trichrome (MT), immunohistochemistry (IHC), H3Ace images at ×200 magnification. It refers to: D: Dentin; P: Periodontal ligament; A: Alveolar bone (n = 3). (**C**) Quantitative analysis of nuclei morphology and H3Ace by histology images. Occlusal force induced increase nuclei aspect ratio and H3Ace expression compared to extrusion group. $^{*}P < 0.05$, or $^{****}P < 0.0001$ by Student's t *t*-test. Ctrl; extrusion group, ST; normal, non-treated.

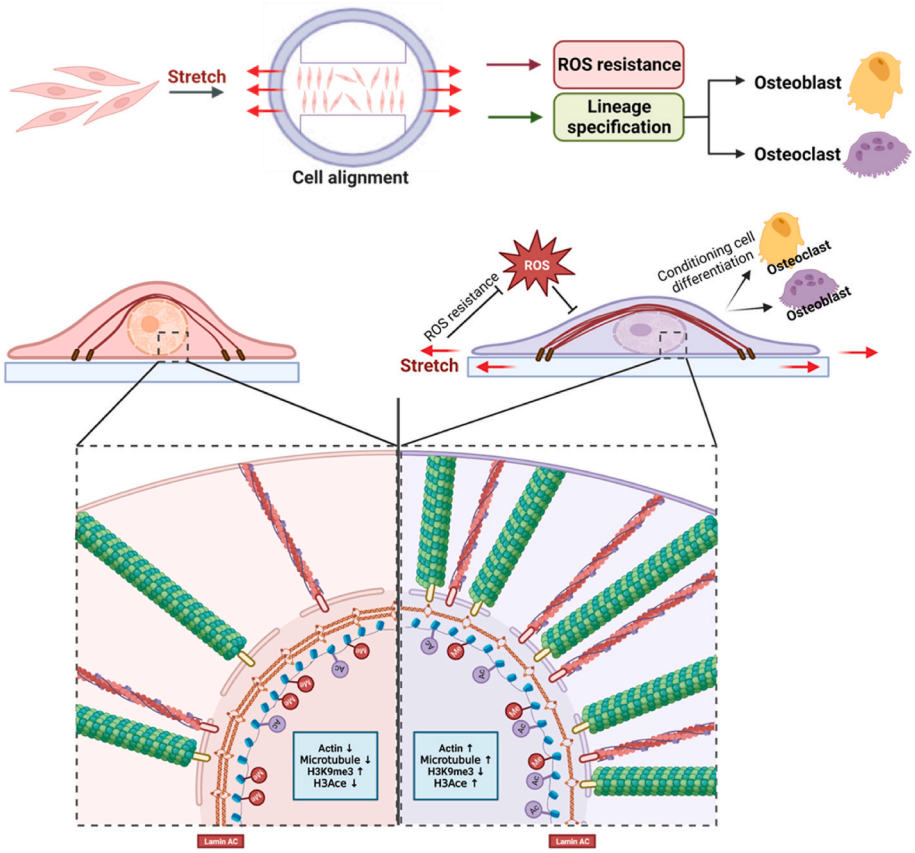

Fig. 8. Mechanical stretch regulates reactive oxygen species (ROS) resistance and lineage specification in periodontal ligament (PDL) cells. Mechanical stretch led to cell alignment via actin and tubulin reorganization, which increased Histone 3 acetylation levels. These epigenetic modifications enhanced gene transcription and provided ROS resistance by promoting an open chromatin state. Additionally, mechanical stretch affected lineage specification, inducing PDL cells into the osteoclast and osteoblast pathways. H3Ace; histone 3 Acetylation, H3K9me3; histone H3 lysine 9 trimethylation, Ac; acetylation, Me; methylation.

Blebbistatin (100 μM), a myosin II inhibitor; nocodazole (0.5 μM), a microtubule inhibitor; and cytochalasin D (0.5 μM), an actin polymerization inhibitor, were used as the inhibitors in the study (Fig. 6B). The concentration of these inhibitors has been used in previous studies on mechanobiology [63–65]. Results showed no significant difference in H3Ace expression between the group subjected to stretch after treatment with blebbistatin, and cyto D, and the stretch-only group with no inhibitor treatment (DMSO group). However, cells treated with nocodazole decreased H3Ace expression versus the DMSO group. Our previous experiments indicated that chromatin structure transforms into a relaxed state due to stretch, leading to increased gene transcription and activity [66,67]. The observed decrease in H3Ace expression by microtubule inhibitor treatment suggests that microtubules play an important role in mediating epigenetic modifications in response to stretch. Furthermore, we quantitated cell alignment in all groups and observed that cell alignment was disrupted in all groups treated with the inhibitor, indicating that nocodazole treatment resulted in loss of cell alignment and decreased expression of H3Ace (Fig. 6C). These findings furnish critical revelations regarding the physiological adaptations and architectural modulations enacted by PDL cells in response to mechanical loading, thus enhancing comprehension of the mechanistic underpinnings of periodontal tissue homeostasis and pathogenesis. Not only stretching but also various other biophysical cues can affect microtubules. It is known that the stiffness and viscoelasticity of the ECM, as well as compression, can influence microtubules and epigenetics. The study finds that a stiff ECM improves cell movement and growth by affecting microtubules [17]. ECM stiffness was also closely related to the epigenetics of histones in the nucleus [68]. When compression occurs, microtubules play a role in stabilizing the cell [51]. However, further research is needed to determine whether these responses occur in the same way in the PDL.

3.7. *In vivo model of hypo-occlusion induced by tooth extraction*

To recapitulate clinically-relevant mechanical loading *in-vivo*, we utilized a rat hypo-occlusion model to simulate the clinical situation where stretch forces are applied (Fig. 7). We hypothesized that periodontal ligament cells in the normal group, which retained opposing tooth contact, would undergo constant tensile loading. In contrast, the extrusion group lacked opposing tooth stimulation, presumptively experiencing attenuated stretch forces (Fig. 7A). HE staining revealed morphological distinctions between groups, with extruded tissue exhibiting rounded, eccentric nuclei contrasting aligned orientations apparent in normal controls. Quantitative image analyses confirmed reduced nuclear angulation relative to tooth longitudinal axis among ligament cells lacking occlusal forces (Fig. 7B and C). Quantitative morphometric analyses validated these architectural distinctions, with sham group nuclei exhibiting greater aspect ratios. Angular profiles likewise differed between groups. Immunohistochemical evaluation revealed mechanical force-mediated changes in H3Ace mirrored earlier *in vitro* observations (Fig. 7C). There have been *in vivo* experiments using rats to study the mechanical cues applied to the PDL [69,70]. The hypo-occlusion model used in this experiment is a model that induces tooth eruption by extracting the opposing teeth, and it was possible to confirm that hypo-occlusion was disadvantageous for bone regeneration [71]. After the extraction of opposing teeth, extrude force acts on the PDL. In this context, compared to normal situations, the PDL of the tooth without its opposing counterpart experiences the removal of

compressive force, making this situation similar with the *in vitro* stretch conditions of this experiment. However, unlike *in vitro* conditions where the stretch can be precisely controlled, it's challenging to strictly regulate this in *in vivo* scenarios, necessitating further research.

3.8. Mechanical stretch regulates ROS resistance and lineage specification in periodontal ligament cells

In this study, we investigated the integrated effects of mechanical stretch on PDL cells, elucidating stretch-mediated oxidative resistance and differentiation capacity. We identified actin cytoskeletal dynamics, microtubule acetylation, and histone H3 acetylation as interconnected regulators of these multifaceted stretch-induced cellular responses (Fig. 8). Mechanical stretching of PDL cells induced cytoskeletal remodeling and cell realignment, as evidenced by actin and tubulin reorganization. Such morphological and orientational adaptation is a vital mechanotransduction enabling cellular responses to mechanical loading [10,72,73]. Stretch-induced cell realignment further elicited heightened H3Ace, an epigenetic signature linked with transcriptional activation. Such enhancement of H3Ace holds important consequences for oxidative tolerance and cell fate trajectories in mechanically strained PDL cells. Specifically, H3Ace-mediated chromatin relaxation fosters an open chromatic configuration permissive for gene expression. This likely allows upregulation of antioxidant defense genes, thereby bolstering cellular resistance to oxidative damage. Moreover, mechanically-triggered chromatin remodeling and relaxed structure may provide greater accessibility for transcription factors to bind lineage-specific genes, thereby guiding differentiation. Furthermore, H3Ace-mediated chromatin remodeling and transcriptional activation likely sway lineage commitment in mechanically loaded PDL cells. Specifically, stretch-induced expression of osteoclast and osteoblast differentiation genes implies mechanical forces guide PDL cell fate choices. This underscores the prospect of harnessing mechanical cues to direct tissue remodeling trajectories. In conclusion, stretch elicits PDL cells realignment via actin and tubulin cytoskeletal reconfiguration, consequently elevating H3Ace levels that confer oxidative defenses while simultaneously influencing lineage specification. Our integrated findings reveal the multifaceted adaptability of PDL cells to mechanical inputs, eliciting coordinated modifications in focal adhesions, chromatin architecture, viability maintenance, and cell fate trajectories. These mechanistic insights enrich the conceptualization of PDL cells mechanotransduction and portend opportunities for translational innovation in periodontal regenerative engineering paradigms.

CRediT authorship contribution statement

Han-Jin Bae: Writing – original draft, Visualization, Validation, Investigation, Formal analysis, Data curation, Conceptualization. **Seong-Jin Shin:** Writing – original draft, Validation, Formal analysis, Data curation. **Seung Bin Jo:** Validation, Data curation. **Cheng Ji Li:** Validation, Data curation. **Dong-Joon Lee:** Writing – review & editing. **Jun-Hee Lee:** Writing – review & editing. **Hae-Hyoung Lee:** Writing – review & editing. **Hae-Won Kim:** Supervision, Funding acquisition. **Jung-Hwan Lee:** Writing – review & editing, Supervision, Funding acquisition, Conceptualization.

Declaration of competing interest

The authors declare that they have no known competing financial interests or personal relationships that could have appeared to influence the work reported in this paper.

Data availability

Data will be made available on request.

Acknowledgment

This work was supported by (NRF) grants, Republic of Korea (2021R1A5A2022318, 2019R1A6A1A11034536, RS-2023-00247485) and Dankook University (Priority Institute Support Program in 2024).

Appendix A. Supplementary data

Supplementary data to this article can be found online at https://doi.org/10.1016/j.mtbio.2024.101050.

References

[1] J.H. Lee, D.H. Kim, H.H. Lee, H.W. Kim, Role of nuclear mechanosensitivity in determining cellular responses to forces and biomaterials, Biomaterials 197 (2019) 60–71, https://doi.org/10.1016/j.biomaterials.2019.01.010.
[2] Y. Shou, et al., Dynamic stimulations with bioengineered extracellular matrix-mimicking hydrogels for mechano cell reprogramming and therapy, Adv. Sci. 10 (2023) e2300670, https://doi.org/10.1002/advs.202300670.
[3] H.X. Du, et al., Tuning immunity through tissue mechanotransduction, Nat. Rev. Immunol. 23 (2023) 174–188, https://doi.org/10.1038/s41577-022-00761-w.
[4] S. Kim, M. Uroz, J.L. Bays, C.S. Chen, Harnessing mechanobiology for tissue engineering, Dev. Cell 56 (2021) 180–191, https://doi.org/10.1016/j.devcel.2020.12.017.
[5] D.H. Kim, P.K. Wong, J. Park, A. Levchenko, Y. Sun, Microengineered platforms for cell mechanobiology, Annu. Rev. Biomed. Eng. 11 (2009) 203–233, https://doi.org/10.1146/annurev-bioeng-061008-124915.
[6] K. Wagh, et al., Mechanical regulation of transcription: recent advances, Trends Cell Biol. 31 (2021) 457–472, https://doi.org/10.1016/j.tcb.2021.02.008.
[7] A.P. Liu, O. Chaudhuri, S.H. Parekh, New advances in probing cell-extracellular matrix interactions, Integr. Biol. 9 (2017) 383–405, https://doi.org/10.1039/c6ib00251j.
[8] D.E. Jaalouk, J. Lammerding, Mechanotransduction gone awry, Nat. Rev. Mol. Cell Biol. 10 (2009) 63–73, https://doi.org/10.1038/nrm2597.
[9] X. Pang, et al., Targeting integrin pathways: mechanisms and advances in therapy, Signal Transduct. Targeted Ther. 8 (2023) 1, https://doi.org/10.1038/s41392-022-01259-6.
[10] F. Martino, A.R. Perestrelo, V. Vinarsky, S. Pagliari, G. Forte, Cellular mechanotransduction: from tension to function, Front. Physiol. 9 (2018) 824, https://doi.org/10.3389/fphys.2018.00824.
[11] K.A. Jansen, P. Atherton, C. Ballestrem, Mechanotransduction at the cell-matrix interface, Semin. Cell Dev. Biol. 71 (2017) 75–83, https://doi.org/10.1016/j.semcdb.2017.07.027.
[12] P. Han, G.A. Gomez, G.N. Duda, S. Ivanovski, P.S.P. Poh, Scaffold geometry modulation of mechanotransduction and its influence on epigenetics, Acta Biomater. 163 (2023) 259–274, https://doi.org/10.1016/j.actbio.2022.01.020.
[13] X.P. Di, et al., Cellular mechanotransduction in health and diseases: from molecular mechanism to therapeutic targets, Signal Transduct Tar 8 (2023), https://doi.org/10.1038/s41392-023-01501-9.
[14] R. Joshi, S.B. Han, W.K. Cho, D.H. Kim, The role of cellular traction forces in deciphering nuclear mechanics, Biomater. Res. 26 (2022), https://doi.org/10.1186/s40824-022-00289-z.
[15] K. Wagh, et al., Mechanical regulation of transcription: recent advances, Trends Cell Biol. 31 (2021) 457–472, https://doi.org/10.1016/j.tcb.2021.02.008.
[16] M. Maurer, J. Lammerding, The driving force: nuclear mechanotransduction in cellular function, fate, and disease, Annu. Rev. Biomed. Eng. 21 (2019) 443–468, https://doi.org/10.1146/annurev-bioeng-060418-052139.
[17] J. Chang, et al., Cell volume expansion and local contractility drive collective invasion of the basement membrane in breast cancer, Nat. Mater. (2023), https://doi.org/10.1038/s41563-023-01716-9, 10.1038/s41563-023-01716-9.
[18] R. LaCanna, et al., Yap/Taz regulate alveolar regeneration and resolution of lung inflammation, J. Clin. Invest. 129 (2019) 2107–2122, https://doi.org/10.1172/Jci125014.
[19] S.M. Park, et al., Cyclic stretch promotes cellular reprogramming process through cytoskeletal-nuclear mechano-coupling and epigenetic modification, Adv. Sci. (2023), https://doi.org/10.1002/advs.202303395, 10.1002/advs.202303395.
[20] R.K. Singh, et al., Coordinated biophysical stimulation of MSCs via electromagnetized Au-nanofiber matrix regulates cytoskeletal-to-nuclear mechanoresponses and lineage specification, Adv. Funct. Mater. (2023) 202304821, https://doi.org/10.1002/adfm.202304821, 10.1002/adfm.
[21] M.M. Nava, et al., Heterochromatin-driven nuclear softening protects the genome against mechanical stress-induced damage, Cell 181 (2020) 800, https://doi.org/10.1016/j.cell.2020.03.052.
[22] F. Mohebichamkhorami, et al., Periodontal ligament stem cells as a promising therapeutic target for neural damage, Stem Cell Res. Ther. 13 (2022), https://doi.org/10.1186/s13287-022-02942-9.
[23] A.A. Volponi, Y. Pang, P.T. Sharpe, Stem cell-based biological tooth repair and regeneration, Trends Cell Biol. 20 (2010) 715–722, https://doi.org/10.1016/j.tcb.2010.09.012.
[24] Z.Q. Zhao, et al., Periodontal ligament stem cell-based bioactive constructs for bone tissue engineering, Front. Bioeng. Biotechnol. 10 (2022), https://doi.org/10.3389/fbioe.2022.1071472.

[25] W.J. Zhu, M. Liang, Periodontal ligament stem cells: current status, concerns, and future prospects, Stem Cell. Int. 2015 (2015), https://doi.org/10.1155/2015/972313.

[26] Y. Li, Q. Zhan, M.Y. Bao, J.R. Yi, Y. Li, Biomechanical and biological responses of periodontium in orthodontic tooth movement: up-date in a new decade, Int. J. Oral Sci. 13 (2021), https://doi.org/10.1038/s41368-021-00125-5.

[27] M.A. Listgarten, Nature of periodontal diseases: pathogenic mechanisms, J. Periodontal. Res. 22 (1987) 172–178, https://doi.org/10.1111/j.1600-0765.1987.tb01560.x.

[28] A.R. El-Awady, et al., Human periodontal ligament fibroblast responses to compression in chronic periodontitis, J. Clin. Periodontol. 40 (2013) 661–671, https://doi.org/10.1111/jcpe.12100.

[29] A.S. Yap, K. Duszyc, V. Viasnoff, Mechanosensing and mechanotransduction at cell-cell junctions, Csh Perspect Biol 10 (2018), https://doi.org/10.1101/cshperspect.a028761.

[30] Y. Kudo, et al., Establishment of human cementifying fibroma cell lines by transfection with temperature-sensitive simian virus-40 T-antigen gene and hTERT gene, Bone 30 (2002) 712–717, https://doi.org/10.1016/s8756-3282(02)00689-0.

[31] D.J. Lee, et al., Bio-implant as a novel restoration for tooth loss, Sci Rep-Uk 7 (2017), https://doi.org/10.1038/s41598-017-07819-z. ARTN7414.

[32] B. Langmead, S.L. Salzberg, Fast gapped-read alignment with Bowtie 2, Nat. Methods 9 (2012) 357–359, https://doi.org/10.1038/nmeth.1923.

[33] A.R. Quinlan, I.M. Hall, BEDTools: a flexible suite of utilities for comparing genomic features, Bioinformatics 26 (2010) 841–842, https://doi.org/10.1093/bioinformatics/btq033.

[34] R.C. Gentleman, et al., Bioconductor: open software development for computational biology and bioinformatics, Genome Biol. 5 (2004) R80, https://doi.org/10.1186/gb-2004-5-10-r80.

[35] B.D. Riehl, J.H. Park, I.K. Kwon, J.Y. Lim, Mechanical stretching for tissue engineering: two-dimensional and three-dimensional constructs, Tissue Eng., Part B 18 (2012) 288–300, https://doi.org/10.1089/ten.TEB.2011.0465.

[36] K. Chen, et al., Role of boundary conditions in determining cell alignment in response to stretch, Proc. Natl. Acad. Sci. U. S. A. 115 (2018) 986–991, https://doi.org/10.1073/pnas.1715059115.

[37] T. de Jong, A.D. Bakker, V. Everts, T.H. Smit, The intricate anatomy of the periodontal ligament and its development: lessons for periodontal regeneration, J. Periodontal. Res. 52 (2017) 965–974, https://doi.org/10.1111/jre.12477.

[38] H.F. Rios, et al., Periostin is essential for the integrity and function of the periodontal ligament during occlusal loading in mice, J. Periodontol. 79 (2008) 1480–1490, https://doi.org/10.1902/jop.2008.070624.

[39] S. Nitsch, L.Z. Shahidian, R. Schneider, Histone acylations and chromatin dynamics: concepts, challenges, and links to metabolism, EMBO Rep. 22 (2021), https://doi.org/10.15252/embr.202152774.

[40] W.W. Tee, D. Reinberg, Chromatin features and the epigenetic regulation of pluripotency states in ESCs, Development 141 (2014) 2376–2390, https://doi.org/10.1242/dev.096982.

[41] M.M. Nava, et al., Heterochromatin-driven nuclear softening protects the genome against mechanical stress-induced damage, Cell 181 (2020) 800–817 e822, https://doi.org/10.1016/j.cell.2020.03.052.

[42] S. Cai, et al., Regulation of cytoskeletal mechanics and cell growth by myosin light chain phosphorylation, Am. J. Physiol. 275 (1998) C1349–C1356, https://doi.org/10.1152/ajpcell.1998.275.5.C1349.

[43] T. Svitkina, The actin cytoskeleton and actin-based motility, Cold Spring Harbor Perspect. Biol. 10 (2018), https://doi.org/10.1101/cshperspect.a018267.

[44] Y. Wu, Y. Ou, C. Liao, S. Liang, Y. Wang, High-throughput sequencing analysis of the expression profile of microRNAs and target genes in mechanical force-induced osteoblastic/cementoblastic differentiation of human periodontal ligament cells, Am J Transl Res 11 (2019) 3398–3411.

[45] X. Zhang, Z. Zhao, Y. Chen, X. Han, Y. Jie, Extracellular vesicles secreted by human periodontal ligament induced osteoclast differentiation by transporting miR-28 to osteoclast precursor cells and further promoted orthodontic tooth movement, Int. Immunopharm. 113 (2022) 109388, https://doi.org/10.1016/j.intimp.2022.109388.

[46] J. Zhou, et al., Mechanism of focal adhesion kinase mechanosensing, PLoS Comput. Biol. 11 (2015) e1004593, https://doi.org/10.1371/journal.pcbi.1004593.

[47] J. Seong, N. Wang, Y.X. Wang, Mechanotransduction at focal adhesions: from physiology to cancer development, J. Cell Mol. Med. 17 (2013) 597–604, https://doi.org/10.1111/jcmm.12045.

[48] D. Ilic, et al., Reduced cell motility and enhanced focal adhesion contact formation in cells from FAK-deficient mice, Nature 377 (1995) 539–544, https://doi.org/10.1038/377539a0.

[49] D.A. Fletcher, R.D. Mullins, Cell mechanics and the cytoskeleton, Nature 463 (2010) 485–492, https://doi.org/10.1038/nature08908.

[50] L. Eshun-Wilson, et al., Effects of alpha-tubulin acetylation on microtubule structure and stability, Proc. Natl. Acad. Sci. U. S. A. 116 (2019) 10366–10371, https://doi.org/10.1073/pnas.1900441116.

[51] Y. Li, et al., Compressive forces stabilize microtubules in living cells, Nat. Mater. 22 (2023) 913–924, https://doi.org/10.1038/s41563-023-01578-1.

[52] A.J. Bannister, T. Kouzarides, Regulation of chromatin by histone modifications, Cell Res. 21 (2011) 381–395, https://doi.org/10.1038/cr.2011.22.

[53] Y. Gruenbaum, R. Foisner, Lamins: nuclear intermediate filament proteins with fundamental functions in nuclear mechanics and genome regulation, Annu. Rev. Biochem. 84 (2015) 131–164, https://doi.org/10.1146/annurev-biochem-060614-034115.

[54] K.L. Wilson, R. Foisner, Lamin-binding proteins, Cold Spring Harbor Perspect. Biol. 2 (2010) a000554, https://doi.org/10.1101/cshperspect.a000554.

[55] T. Dechat, et al., Nuclear lamins: major factors in the structural organization and function of the nucleus and chromatin, Genes Dev. 22 (2008) 832–853, https://doi.org/10.1101/gad.1652708.

[56] C. Sun, et al., Effect of tension on human periodontal ligament cells: systematic review and network analysis, Front. Bioeng. Biotechnol. 9 (2021) 695053, https://doi.org/10.3389/fbioe.2021.695053.

[57] R. Bhuyan, et al., Periodontitis and its inflammatory changes linked to various systemic diseases: a review of its underlying mechanisms, Biomedicines 10 (2022), https://doi.org/10.3390/biomedicines10102659.

[58] M. Usui, et al., Mechanism of alveolar bone destruction in periodontitis - periodontal bacteria and inflammation, Jpn Dent Sci Rev 57 (2021) 201–208, https://doi.org/10.1016/j.jdsr.2021.09.005.

[59] H.M. Ko, et al., Inhibitory effect of C-X-C motif chemokine ligand 14 on the osteogenic differentiation of human periodontal ligament cells through transforming growth factor-beta1, Arch. Oral Biol. 115 (2020) 104733, https://doi.org/10.1016/j.archoralbio.2020.104733.

[60] A. Hosoya, et al., Immunohistochemical localization of alpha-Smooth muscle actin during rat molar tooth development, J. Histochem. Cytochem. 54 (2006) 1371–1378, https://doi.org/10.1369/jhc.6A6980.2006.

[61] B. Kinner, M. Spector, Expression of smooth muscle actin in osteoblasts in human bone, J. Orthop. Res. 20 (2002) 622–632, https://doi.org/10.1016/S0736-0266(01)00145-0.

[62] B.G. Matthews, et al., alphaSMA osteoprogenitor cells contribute to the increase in osteoblast numbers in response to mechanical loading, Calcif. Tissue Int. 106 (2020) 208–217, https://doi.org/10.1007/s00223-019-00624-y.

[63] N.Y. Chen, et al., Fibroblasts lacking nuclear lamins do not have nuclear blebs or protrusions but nevertheless have frequent nuclear membrane ruptures, Proc. Natl. Acad. Sci. U. S. A. 115 (2018) 10100–10105, https://doi.org/10.1073/pnas.1812622115.

[64] M.W.G. Schneider, et al., A mitotic chromatin phase transition prevents perforation by microtubules, Nature 609 (2022) 183–190, https://doi.org/10.1038/s41586-022-05027-y.

[65] M. Shutova, C. Yang, J.M. Vasiliev, T. Svitkina, Functions of nonmuscle myosin II in assembly of the cellular contractile system, PLoS One 7 (2012) e40814, https://doi.org/10.1371/journal.pone.0040814.

[66] Y. Song, J. Soto, S. Li, Mechanical regulation of histone modifications and cell plasticity, Curr. Opin. Solid State Mater. Sci. 24 (2020), https://doi.org/10.1016/j.cossms.2020.100872.

[67] J.S. Butler, S.Y. Dent, The role of chromatin modifiers in normal and malignant hematopoiesis, Blood 121 (2013) 3076–3084, https://doi.org/10.1182/blood-2012-10-451237.

[68] S. Nemec, K.A. Kilian, Materials control of the epigenetics underlying cell plasticity, Nat. Rev. Mater. 6 (2021) 69–83, https://doi.org/10.1038/s41578-020-00238-z.

[69] J. Xu, et al., Role of autophagy in the periodontal ligament reconstruction during orthodontic tooth movement in rats, J. Dent. Sci. 15 (2020) 351–363, https://doi.org/10.1016/j.jds.2020.02.005.

[70] T. Hiraga, T. Ninomiya, A. Hosoya, M. Takahashi, H. Nakamura, Formation of bone-like mineralized matrix by periodontal ligament cells *in vivo*: a morphological study in rats, J. Bone Miner. Metabol. 27 (2009) 149–157, https://doi.org/10.1007/s00774-009-0039-9.

[71] A. Damanaki, et al., Influence of occlusal hypofunction on alveolar bone healing in rats, Int. J. Mol. Sci. 24 (2023), https://doi.org/10.3390/ijms24119744.

[72] M.N. Andalib, Y. Dzenis, H.J. Donahue, J.Y. Lim, Biomimetic substrate control of cellular mechanotransduction, Biomater. Res. 20 (2016) 11, https://doi.org/10.1186/s40824-016-0059-1.

[73] H. Wolfenson, B. Yang, M.P. Sheetz, Steps in mechanotransduction pathways that control cell morphology, Annu. Rev. Physiol. 81 (2019) 585–605, https://doi.org/10.1146/annurev-physiol-021317-121245.